Evaluation of Treatment Response to Radiotherapy in Head and Neck Cancer with Fluorine-18 Fluorodeoxyglucose

Heikki Minn, Robert Paul, and Aapo Ahonen

Departments of Radiotherapy, Medicine, and Radiology, Division of Nuclear Medicine, University Central Hospital of Turku; and Turku Medical Cyclotron Project, Turku; Finland

Nineteen patients with malignant head and neck tumors were imaged before and during radiation therapy with ^{18}F-2-fluoro-2-deoxy-D-glucose (FDG) to study the effect of radiotherapy (RT) on FDG uptake. All tumor images were FDG-positive before treatment. After RT, a decrement of tumor FDG uptake was found in all but two patients; these were nonradioresponders. There was a significant decrement ($p < 0.001$) in uptake ratios after irradiation of 30 ± 5 Gy among the radioresponsive (CR + PR) but not among the radioresistant (NC + PD) tumors. The administered dose of RT correlated ($r = 0.47$, $p < 0.05$) with the decrement in FDG activity among the CR + PR but not among the NC + PD patients. The biologic half-life of FDG radioactivity in tumor tissue was evaluated by dynamic scintigraphy. A change in the half-life of FDG toward the value observed in normal tissue was associated with treatment response. The results suggest that FDG imaging can be used for follow-up of RT in patients with head and neck cancer.

J Nucl Med 29:1521–1525, 1988

It remains difficult to predict the outcome of radiotherapy (RT) of cancer despite major progress in diagnosis, treatment planning, and therapeutic modalities. Tumor size, morphology, histology, and other presently used clinical methods for assessing tumor radiocurability are relatively nonspecific and imprecise (*1*). Consequently, it has become increasingly important to develop predictive methods based on individual tumor properties. Several radiobiologic factors which influence the radiation response have been identified (*2*), but their use in clinical practice is far from established. Positron emission tomography (PET) has made it possible to study the biochemical changes of cancer tissue and PET may make it possible to study the effect of treatment on the metabolism in vivo (*3*). Glucose and amino acid metabolism are maybe the most fruitful compounds worth studying in this context (*4,5*).

Fluorine-18-2-fluoro-2-deoxy-D-glucose (FDG) is well suited for studies on glycolysis in man (*6*). The metabolic pathways of the tracer are known (*7*). The application of the Sokoloff-Phelps method for FDG (*6, 8*) may be used to study cancer, though more data on kinetic, enzymatic and metabolic factors on different tumors are needed for exact validation of the model for malignant tissue. However, FDG may be used for successful imaging of human tumors, like cerebral gliomas (*9*), liver metastases from colon carcinoma (*10*), hepatoma (*11*), thyroid cancer (*12*), and primary and secondary bone tumors (*13*).

Head and neck cancer is suitable for evaluating radiotherapeutic effects because of easy staging and follow-up of treatment. Most of the head and neck cancers respond well to radiation treatment. Recently, 5-yr survival rates of ~20% have been reported for patients with cervical node metastases treated with RT, with a maximum of 50% for the nasopharynx tumors (*14*). However, inherent radioresistance is a common phenomenon and usually at least 2 yr of follow-up is needed before any conclusions of the potential cure can be made (*15*).

RT is laborious and exhausting both for the patient and the treatment unit and thus early recognition of responders and nonresponders would be useful. Further benefit would be gained from a method identifying those patients who could be cured by radical RT. This work was carried out in order to study if imaging with FDG could be used for identifying treatment responders

Received Sept. 22, 1987; revision accepted Mar. 28, 1988.

For reprints contact: Heikki Minn, MD, Dept. of Radiotherapy, University of Turku, SF-20520 Turku, Finland.

already during the course of RT of head and neck tumors.

PATIENTS AND METHODS

Patients

Permission for the use of FDG was obtained from the Ethical Committee of the Turku University Central Hospital and the patients gave oral informed consent. Twenty-one patients with a malignant tumor of the head and neck region were entered in the study. Two patients were excluded from the final study for logistic reasons. Of the remaining 19 patients, 16 had a primary carcinoma of the head and neck region, two lymphomas limited to a single site and one a soft-tissue metastasis of left mandibular arch from prostatic cancer. The diagnosis and the grade of tumor differentiation were determined histologically according to the criteria stated by WHO (*16*). The size of the tumors ranged from 2 × 2 × 2 cm to 3 × 5 × 10 cm.

All patients were referred for megavoltage RT consisting of daily fractions of 2.0 Gy (10.0 Gy weekly), and received ~32 Gy in three weeks. At this stage, the outcome of RT was assessed clinically and laryngoscopically, and response was recorded as complete response (CR), partial response (PR), no change (NC) and progressive disease (PD) according to standard criteria (*17*). After this, three patients were operated on and received postoperative RT; 11 were given radical RT up to 60–70 Gy and for five patients the treatment remained palliative.

FDG Imaging

FDG was synthesized at the Turku Medical Cyclotron Laboratory as described (*18*). Imaging was performed with a conventional gamma camera (Searle Pho Gamma V, Siemens Medical Systems, Iselin, NJ) equipped with a 1-in crystal and a special collimator for 511 keV photons. The patients received doses of FDG ranging from 2 to 8 mCi intravenously as a bolus and imaging was started immediately after injection. One-minute frames were collected for 30 min and were followed by a static image between 30–55 min after the injection. This image of ~200,000 counts was considered to represent the steady state phase of the study. All data was collected and analyzed with a PDP 11/34 computer (Digital Equipment Corp. Ltd., Maynard, MA) using the GAMMA-11 software. Each patient was imaged with FDG before RT and again after a tumor dose of ~30 Gy (mean 30 ± 5 Gy).

Data Analysis

Each static image was analyzed with conventional region of interest (ROI) techniques by choosing the contralateral or, in the case of nasopharynx tumors, adjacent normal tissue, as a reference for the tumor hot spot. When possible, several ROIs were chosen from the tumor in the case of difference between accumulations of the primary tumor and the neck metastases or when the tumor included necrotic areas. In these cases, the highest accumulation was used for analysis. The tumor-to-normal tissue activity contrast ratio (TCR) was determined from the ratio of the time-integrated sums of counts of the tumor and the reference normal ROI. The static images were also analyzed visually by an experienced nuclear medicine physician (AA). The intensity of the accumulation was graded into five groups on a visual scale ranging from no accumulation (grade 0), to equivocal (grade 1), slight but definite (grade 2), moderate (grade 3), and intensive accumulation (grade 4).

The dynamic scintigraphies were analyzed with single exponential or biexponential functions of the form $y(t) = Ae^{at}$ or $y(t) = Ae^{at} + Be^{bt}$ using least squares and curve peeling techniques. The biologic half-life ($T_{1/2}$) of FDG in a tumor ROI was thus 0.693/a for the fast, and 0.693/b for the slow component, respectively (*19*). The fast component was predominant for only 2–3 min after the injection of FDG, when the activity in the ROI increased steeply. Due to the great variability in the fast component (which was thought to represent flow rather than metabolism), only the slow one was considered when biexponential functions were best fits. A $T_{1/2}$ of ≥350 min without regard for increase or decrease was arbitrarily regarded as level (L). Half-times less than this were regarded as increasing (I) or decreasing (D), depending on the direction of the curve.

Statistical Methods

Student's t-test for pairwise comparisons and Pearson's coefficient of correlation were used.

RESULTS

Static Study

All the pretherapeutic static FDG images showed uptake in the tumor, but the intensity of the accumulation varied considerably. The calculated TCRs ranged from 2.7 to 1.3 (mean 1.88 ± 0.42). The TCR among the well differentiated (G_1, n = 9) tumors was 1.78 ± 0.40 and poorly differentiated (G_3, n = 8) tumors 1.84 ± 0.54 (N.S.), while tumors with a maximum diameter of ≥5 cm had a TCR of 1.97 ± 0.47 (n = 11) and tumors with a diameter of 2 to 5 cm, 1.76 ± 0.30 (n = 8, N.S.).

As a consequence of radiotherapy, a decrement of FDG uptake was seen in all but two patients and both of these had G_1 tumors. In addition, these two patients were also nonresponders. The posttreatment TCRs ranged from 2.0 to 1.0 (mean 1.31 ± 0.27). The average TCR was significantly smaller ($p < 0.001$) after RT than before RT. For the clinical responders (CR + PR, n = 13), the mean pretreatment TCR was 1.91 ± 0.40, and after 31 ± 6 Gy of irradiation 1.17 ± 0.14 ($p < 0.001$). For the nonresponders (NC + PD, n = 6) the pretreatment TCR was 1.83 ± 0.46, and after 30 ± 3 Gy of irradiation, 1.60 ± 0.25 (N.S.) (Fig. 1). In at least four patients the TCR decrement preceded clinical regression of the irradiated tumor. There was a weak but significant ($r = 0.47$, $p < 0.05$) correlation between the administered dose of RT and the decrement in the TCR among responders; no such correlation was seen among the nonresponders ($r = 0.24$, N.S.).

Dynamic study. The decay corrected time-activity curves were divided into three subgroups (D, L, and I)

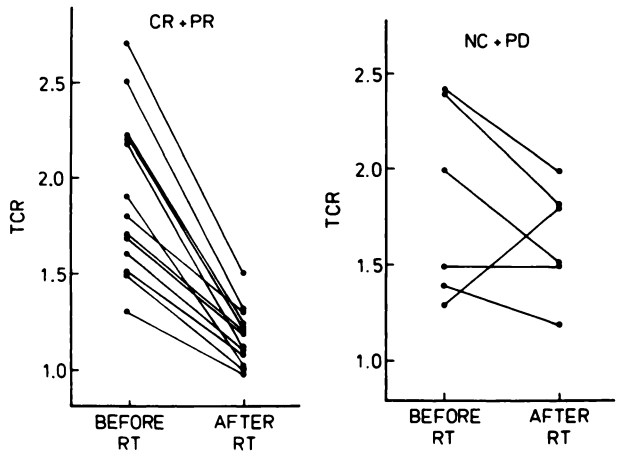

FIGURE 1
FDG uptake before radiotherapy (RT) and after 30 Gy of irradiation among 13 radioresponsive (CR + PR) and six radioresistant (NC + PD) head and neck tumors.

according to their biologic half-lives (see Methods). Examples of the dynamic curves are shown in Figure 2. The D curve resembled that of the contralateral normal tissue; the biologic (decay corrected) $T_{1/2}$ of normal tissue was 150 ± 95 min. Among the responders there were 8/13 (62%) whose curve shape changed from the I or L to the D type, while the respective change among the nonresponders was 2/6 (33%, Table 1). There were 6/19 patients whose curve shape remained unchanged; only two patients showed a change towards

FIGURE 2

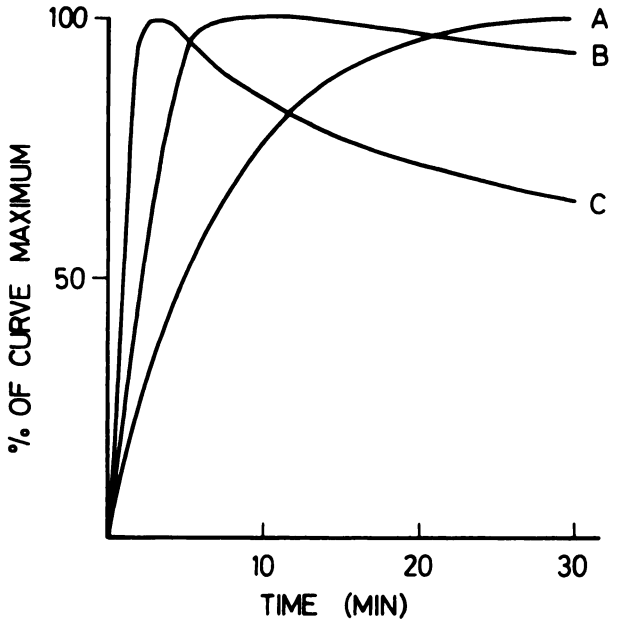

Dynamic FDG decay corrected time-activity curves (0–30 min) demonstrating three types of curve shapes: A) constantly increasing, B) level, and C) constantly decreasing, all before RT.

TABLE 1
Dynamic FDG Time-Activity Curve Shape Before RT and After 30 Gy of Irradiation Among 13 Radioresponsive (CR+PR) and Six Radioresistant (NC+PD) Head and Neck Tumors

	CR+PR		NC+PD	
Curve-type	Before RT	After RT	Before RT	After RT
Increasing	6	—	2	3
Level	3	1	2	1
Decreasing	4	12	2	2

an I type of curve and these were the same nonresponders as mentioned in the preceding paragraph.

Visual Interpretation

The visual grading of the static scintigrams was generally in accordance with the quantitative analysis. Pretherapeutically, 11/19 (58%) of the tumors were scored as grade 4 and 4/19 (21%) as grade 3 group and the mean TCRs for these groups were 2.11 ± 0.37 and 1.75 ± 0.29, respectively. The accumulation of FDG in the tumor decreased by 1–3 grade units among all CR + PR patients; among the NC + PD group 4/6 patients had a decrement of one grade unit, one had a stable scintigram and one an increase of three grade units (Patient C, Fig. 3). Some typical scintigrams of patients with and without response are shown in Figure 3.

DISCUSSION

The present study shows that head and neck cancer may be well imaged with [^{18}F]FDG and a specially collimated gamma-camera, although the visualization of necrotic tumors may be hampered because the uptake is limited to viable tumor cells (*20*). In addition, low-grade malignant tumors may be missed in FDG scintigraphy due to their low glycolytic activity which is close to the normal tissue (*9*). Although the FWHM of our specially collimated gamma camera is ~20 mm, the sensitivity for (viable) tumor detection was 100% in our series of 19 patients. This compares favorably with imaging of head and neck cancer by ^{67}Ga, where detection rates from 33% to 86% have been reported (*21*).

There are only few studies on the effects of RT on FDG uptake in malignant tissue. Clinical reports of irradiated malignant gliomas suggest that FDG imaging may be used for differentiating radiation necrosis from relapsing cancer (*22*). Abe et al. (*23*) studied experimental murine tumors with FDG during irradiation and found decrements of tumor uptake in radiosensitive FM3A mammary carcinoma and AH109A hepatoma, whereas in radiation resistant MM48 mammary carcinoma the uptake remained constant. In addition, they found that tumor volume does not affect FDG accu-

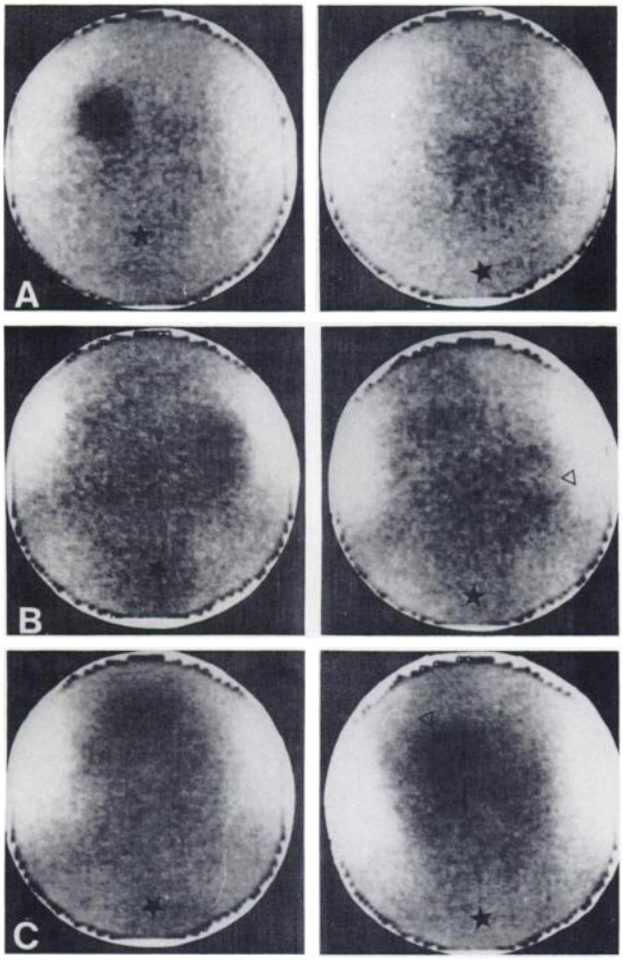

FIGURE 3
FDG images of three patients with head and neck tumors, before RT (right) and after tumor dose of 30 Gy (left; * = suprasternal notch, all ap-projections): A) stage IA high grade (G_3) lymphoma in the right neck shows a complete resolution (CR) of the tumor B) metastatic lymph node from epiglottic cancer in the left neck: a hot spot becomes obscure due to the central necrosis of the tumor (arrowhead) after irradiation, but the radiation response remains poor (NC) C) widespread squamous cancer of tongue: the pretherapeutic tumor FDG uptake is equivocal; during irradiation, the disease progressed clinically (PD), and after 25 Gy of RT an intensive uptake in tumor (arrowhead) could be detected.

mulation and that FDG uptake began to decrease even while tumor volume was still almost unchanged. They concluded that the decreased uptake ratio was not due to the loss of tumor volume but to the cell killing effect of radiation. This was in agreement with another experimental tumor study with [^{3}H]deoxyglucose, where the reduction of uptake in tumor after irradiation was found to correlate with the tissue viability rather than tumor weight and size (*24*).

In our study, the difference between the uptake decrement in clinical radioresponders (CR + PR) and nonresponders (NC + PD) was significant ($p < 0.001$). Further, the only patient with clinical progression during RT was the only one in which an increase of FDG uptake could also be observed. Yet the individual TCR values calculated from planar images cannot be used per se for quantitative evaluation of the metabolic rate of glucose. In the present study the TCRs were corrected neither for blood activity nor for activity from under- or overlying tissue, which may influence the interpretation especially in the case of small, deep-seated tumors. Therefore, a PET FDG study for the validation of these observations is highly desirable.

The changes in dynamic curves were also more prominent among responders than nonresponders, where 62% vs. 33% of the patients had a change toward the normal tissue type of the activity curve of FDG. If the patients where the initial curve types of the tumor ROIs showed a D pattern are excluded the respective values are 100% and 50%. Still, there is a wide variation in the $T_{1/2}$'s of the time-activity curves in normal tissue ($T_{1/2}$ = 150 ± 95 min). As to our $T_{1/2}$ values, neither blood nor tissue background activity was calculated. Moreover, the biologic $T_{1/2}$ of a radiopharmaceutical compound depends on microenvironmental factors such as blood supply, pH, tissue vitality and proliferation, and enzyme kinetics. Thus the absolute $T_{1/2}$'s have to be regarded with caution, while the shape of the curve (I, L, or D) may be more informative.

This study indicates that a rapid reduction of FDG uptake in cancer tissue during RT indicates a good radiation response of head and neck tumors after a dose of 30 Gy. In this series the change was independent of tumor differentiation, although a more uniform uptake decrement could be recorded among G_3 tumors than G_1 tumors. An increase in the uptake of FDG or a persistent abnormal time-activity curve in the dynamic scintigram during RT appears to be a sign of an unfavorable response. Thus, the early recognition of responders and nonresponders may become possible by serial FDG imaging. Whether it can predict radiocurability cannot be determined in this study due to the short follow-up time of the patients.

We conclude that FDG imaging provides a useful method to follow treatment response during RT in head and neck cancer. Its validity in predicting local tumor control and long-time survival needs further investigation and has to be related to other prognostic factors. Moreover, the biologic mechanism by which FDG uptake diminishes during irradiation is not yet clearly understood and needs to be clarified.

ACKNOWLEDGMENTS

The authors thank the staff of The Turku Medical Cyclotron Laboratory for production of [^{18}F]FDG, and S. Parviainen, PhLic, for assistance with the dynamic data analysis. This work has been made possible by funding from the Academy of Finland and the Cancer Foundation of Finland.

REFERENCES

1. Peters LJ, Brock WA, Johnson T, et al. Potential methods for predicting tumor radiocurability. *Int J Radiat Oncol Biol Phys* 1986; 12:459–467.
2. Russo A, Mitchell J, Kinsella T, et al. Determinants of radiosensitivity. *Semin Oncol* 1985; 12:332–349.
3. Kairento AL, Brown GL, Elmaleh DR, et al. Comparative measurement of regional blood flow, oxygen and glucose utilization in soft tissue tumour of rabbit with positron imaging. *Br J Radiol* 1985; 58:637–643.
4. Patronas NJ, DiChiro G, Kufta C, et al. Prediction of survival in glioma patients by means of positron emission tomography. *J Neurosurg* 1985; 62:816–822.
5. Kubota K, Matsuzawa T, Ito M, et al. Lung tumor imaging by positron emission tomography using C-11-L-methionine. *J Nucl Med* 1985; 26:37–42.
6. Phelps ME, Huang SC, Hoffman EJ, et al. Tomographic measurement of local cerebral glucose metabolic rate in humans with (F-18)2-fluoro-2-deoxy-D-glucose: validation of a method. *Ann Neurol* 1979; 6:371–388.
7. Reivich M, Alavi A, Wolf A, et al. Glucose metabolic rate kinetic model parameter determination in humans: the lumped constants and rate constants for (^{18}F)fluorodeoxyglucose and (^{11}C)deoxyglucose. *J Cereb Blood Flow Metab* 1985; 5:179–192.
8. Sokoloff L, Reivich M, Kennedy C, et al. The (14C)deoxyglucose method for the measurement of local cerebral glucose utilization: theory, procedures, and normal values in the conscious and anesthetized albino rat. *J Neurochem* 1977; 28:897–916.
9. Di Chiro G, DeLaPaz RL, Brooks RA, et al. Glucose utilization of cerebral gliomas measured by (^{18}F)fluorodeoxyglucose and positron emission tomography. *Neurology* 1982; 32:1323–1329.
10. Yonekura Y, Benua RS, Brill AB, et al. Increased accumulation of 2-deoxy-2-(^{18}F)fluorodeoxy-D-glucose in liver metastases from human colon carcinoma. *J Nucl Med* 1982; 23:1133–1137.
11. Paul R, Ahonen A, Nordman E, et al. Imaging of hepatoma with (^{18}F)-fluorodeoxyglucose. *Lancet* 1985; 1:50–51.
12. Joensuu H, Ahonen A, Klemi P. ^{18}F-fluorodeoxyglucose imaging in preoperative diagnosis of thyroid malignancy. *Eur J Nucl Med*: 1988;13:502–506.
13. Ahonen A, Paul R, Aho A, et al. Differential diagnosis of bone tumors using fluorodeoxyglucose and three phase ^{99m}Tc-DPD scanning. In: Nuklearmedizin. Proc. ENMC. Stuttgart-New York, Schattauer Verlag, 1986: 441–443.
14. Bloom HJG. Introduction and overview. Perspectives of multidisciplinary management. In: Bloom HJG, Hanham IWF, Shaw HJ, eds. *Head and neck oncology.* New York: Raven Press, 1986: 1–17.
15. Peters LJ, Fletcher GH. Causes of failure of radiotherapy in head and neck cancer. *Radiotherapy Oncol* 1983; 1:53–63.
16. Shanmugaratnam K, Sobin LH. Histologic typing of upper respiratory tract tumours. Geneva: World Health Organization, 1978.
17. Miller AB, Hoogstraten B, Staquet M, et al. Reporting results of cancer treatment. *Cancer* 1981; 47:207–214.
18. Haaparanta M, Bergman J, Solin O, Roeda D. A remotely controlled system for the routine synthesis of ^{18}F-2-fluoro-2-deoxy-D-glucose. *Nuklearmedizin* 1984;21:(suppl 21):823–826.
19. Paul R, Parviainen S. Dynamic scintigraphy of tumor bearing rats with (^{18}F)-2-fluoro-2-deoxy-D-glucose. *Res Exp Med* 1986; 186:249–258.
20. Kato A, Diksic M, Yamamoto YL, et al. Quantification of glucose utilization in an experimental brain tumor model by the deoxyglucose method. *J Cereb Blood Flow Metab* 1985; 5:108–114.
21. Bekerman C, Hoffer PB, Bitran JD. The role of gallium-67 in the clinical evaluation of cancer. *Semin Nucl Med* 1984; 14:296–323.
22. Patronas NJ, DiChiro G, Brooks RA. Work in progress: (^{18}F)-fluorodeoxyglucose and positron emission tomography in the evaluation of radiation necrosis of the brain. *Radiology* 1982; 144:885–889.
23. Abe Y, Matsuzawa T, Fujiwara T, et al. Assessment of radiotherapeutic effects on experimental tumors using ^{18}F-2-fluoro-2-deoxy-D-glucose. *Eur J Nucl Med* 1986; 12:325–328.
24. Iosilevsky G, Front D, Bettman L, et al. Uptake of gallium-67 citrate and (2-^{3}H)deoxyglucose in the tumor model, following chemotherapy and radiotherapy. *J Nucl Med* 1985; 26:278–282.